IEEE Photonics Journal
An IEEE Photonics Society Publication

Open Access

Physical Layer Security of Hybrid Satellite-FSO Cooperative Systems

Volume 11, Number 1, February 2019

Yun Ai, *Member, IEEE*
Aashish Mathur, *Member, IEEE*
Michael Cheffena
Manav R. Bhatnagar, *Senior Member, IEEE*
Hongjiang Lei, *Member, IEEE*

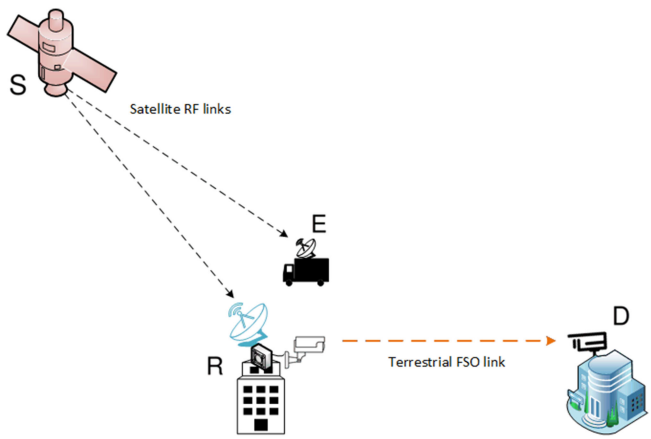

DOI: 10.1109/JPHOT.2019.2892618
1943-0655

Physical Layer Security of Hybrid Satellite-FSO Cooperative Systems

Yun Ai,[1] ***Member, IEEE***, **Aashish Mathur**,[2] ***Member, IEEE***, **Michael Cheffena**,[1] **Manav R. Bhatnagar**,[3] ***Senior Member, IEEE***, **and Hongjiang Lei**,[4] ***Member, IEEE***

[1]Faculty of Engineering, Norwegian University of Science and Technology, 2815 Gjøvik, Norway
[2]Department of Electrical Engineering, Indian Institute of Technology Jodhpur, Jodhpur 342037, India
[3]Department of Electrical Engineering, Indian Institute of Technology - Delhi, New Delhi 110016, India
[4]School of Communication and Information Engineering, Chongqing University of Posts and Telecommunications, Chongqing 400065, China

DOI:10.1109/JPHOT.2019.2892618

Manuscript received October 26, 2008; revised January 7, 2019; accepted January 9, 2019. Date of publication January 16, 2019; date of current version February 1, 2019. The work of Y. Ai and M. Cheffena was supported by the Norwegian University of Science and Technology (NTNU), Norway. The work of M. R. Bhatnagar was supported by the Indo-US Science and Technology Forum (IUSSTF) through Department of Science and Technology (DST) under JCERDC grant-in aid for project titled: UI-ASSIST: US India collaboration for Smart Distribution System with Storage (Ref. No.: IUSSTF/JCER DC-SMART GRIDS AND ENERGY STORAGE/2017). Corresponding author: Yun Ai (e-mail: yun.ai@ntnu.no).

Abstract: In this paper, we study the physical layer secrecy performance of a hybrid satellite and free-space optical (FSO) cooperative system. The satellite links are assumed to follow the shadowed-Rician fading distribution, and the channel of the terrestrial link between the relay and destination is assumed to experience the gamma–gamma fading. For the FSO communications, the effects of different types of detection techniques (i.e., heterodyne detection and intensity modulation with direct detection) as well as the pointing error are considered. We derive exact analytical expressions for the average secrecy capacity and secrecy outage probability (SOP) for both cases of amplify-and-forward (AF) and decode-and-forward (DF) relaying. The asymptotic analysis for the SOP is also conducted to provide more insights on the impact of FSO and satellite channels on secrecy performance. It is found that with the AF with fixed gain scheme, the secrecy diversity order of the investigated system is only dependent on the channel characteristics of the FSO link and the FSO detection type, whereas the secrecy diversity is zero when the relay node employs DF or AF with variable-gain schemes.

Index Terms: Physical layer security, hybrid satellite free-space optical (FSO) cooperative system, land mobile satellite (LMS) channel, secrecy outage probability, average secrecy capacity.

1. Introduction

1.1 Background and Motivations

Satellite systems have been widely used in navigation, broadcasting, and disaster relief due to advantage of providing service over a wide area with high data transmission rate, especially in scenarios where the wired or wireless terrestrial communication systems are not available [1].

However, the availability of satellite signals can be often hindered by the masking effect from the shadowing and obstacles that block the line-of-sight (LoS) communication link between the satellite and a terrestrial user [2]. To overcome the masking effect of satellite communications, hybrid satellite-terrestrial cooperative systems have been developed to take advantage of the relaying technique [2]. The newly founded International Telecommunication Union (ITU-T) Focus Group on Network 2030 forecasts that the convergence of terrestrial and space networks is essential for the future generation communication system to achieve the goal of providing communication service for everyone everywhere at any time [3]. Among different terrestrial communication techniques, optical communication through the atmosphere, i.e., free-space optical (FSO) communication, has gained increasing attention due to its potential as a cost-effective and wide bandwidth solution operating within the unlicensed optical frequency band, relative to the conventional radio frequency (RF) transmission systems [2], [4]–[7].

The hybrid satellite-FSO cooperative system can find applications in a number of scenarios due to its advantages in terms of fast and affordable deployment, wide coverage, and high throughput. For instance, during disaster recovery, the establishment of broadband access for the disaster area is essential. If the terrestrial communication infrastructure is severely damaged, a geostationary satellite with the FSO system can quickly provide broadband communication links to a large amount of users in the disaster area. It is suggested in [8] that in a disaster scenario, transportable cooperative relaying ground stations can be deployed to provide broadband access in the disaster areas; these stations receive satellite signals and then relay the received signals to a masked destination node over the FSO link. The advantages of both satellite and FSO system enable the hybrid satellite-terrestrial cooperative system to provide broadband access with large coverage area in both cost-efficient and fast way. According to the ITU report [9], around half of the global population remain unconnected to the Internet with most of them living in the least developed countries. Therefore, the cost-effective hybrid satellite-FSO solution also serves as a very promising technique to mitigate the digital divide in the least developing countries, which generally have inadequate optical fiber network and wireless network infrastructure [9].

1.2 Related Works and Contributions

Resulting from the inherent nature of satellite broadcasting and its wide coverage area, satellite communications are prone to security threats. The potentially strong computation ability of the eavesdropper makes the traditional satellite communication security approach through the cryptographic protocols in the upper layers not necessarily robust [10], hence security problem should also be addressed from the physical layer perspective by using the randomness and time-varying nature of the radio wave propagation channel [6], [7], [10]–[12]. It is shown through the physical layer security (PLS) theory in [13] that secure information transmission can be achieved when the quality of the eavesdropper's link is inferior to that of the legitimate link. This motivates the research of communication security from the information-theoretic perspective [6], [7], [10], [11], [14]–[17]. The secrecy performance analysis of a mixed RF-FSO system by assuming the RF link undergoing Nakagami-m fading is conducted in [6], which is further extended to the scenario with channel imperfection in [7]. The PLS performance of a mixed RF/FSO dual-hop system is studied in [14] by assuming the RF channels following $\eta - \mu$ fading and the FSO link experiencing $\mathcal{M}$-distributed fading. The secrecy performance of a cognitive satellite-terrestrial network is investigated in [10], where the satellite links are assumed to experience Shadowed-Rician fading and the wireless links undergo Rayleigh fading. In [11], the secrecy outage performance of a land mobile satellite system is investigated, where both the legitimate user and eavesdropper are equipped with multiple antennas and employ the maximal ratio combining scheme. The secrecy performance of a hybrid satellite-terrestrial relay network in the presence of multiple eavesdroppers is analyzed in [15]. It is assumed that the multiple eavesdroppers receive signals from the terrestrial networks. In [16], the performance of robust secure beamforming for the fifth generation (5G) wireless systems operating at millimeter wave frequency and coexisting with a satellite network is studied. The secrecy performance of a cognitive satellite-terrestrial network in the presence of an eavesdropper equipped

with multiple antenna is investigated in [17], where the interference from the mobile base station is purposely introduced to enhance the security of the satellite link.

Motivated by the latest advances in physical layer security analysis [11], [15]–[18] and the potential of the hybrid satellite-FSO system in various scenarios, we study the secrecy performance of satellite-FSO cooperative system for both the cases of amplify-and-forward (AF) and decode-and-forward (DF) relayings in this paper. To the best of the authors' knowledge, the secrecy performance of satellite-FSO cooperative system has not been studied from the physical layer perspective. The conducted analysis in this paper also significantly differs from the other papers on the secrecy performance analysis of satellite-cellular or land mobile satellite systems. On the one hand, FSO propagation channel poses different propagation characteristics compared to the radio frequency links in terms of fading, turbulence, and pointing errors. On the other hand, the good directivity of FSO link ensures that the eavesdropper resort to receive signals from the satellite links while in satellite-cellular systems, the eavesdroppers are more likely to receive signals from the cellular networks since the signals from cellular networks can be stronger. The main contributions of the paper are listed as follows:

- We investigate the secrecy performance of the hybrid satellite-FSO cooperative system under AF and DF relaying strategies. The fading of the satellite link is modeled by the widely used Shadowed-Rician model while the FSO channel fading is modeled by the Gamma-Gamma distribution. Besides the fading effects of the channels, the impact of FSO pointing error and detection technique are taken into consideration in our analysis.
- Contrary to previous work on the secrecy performance of communication systems involving FSO link [6], [7], [12], we derive the exact expression for secrecy outage probability (SOP) in addition to closed-form exact expression for average secrecy capacity (ASC) in the paper.
- To gain more insights on the secrecy performance of the hybrid satellite-FSO communication system, asymptotic SOP analysis of the investigated system is conducted with the secrecy diversity order being derived. The impact of the FSO detection types on the achievable secrecy diversity order is also analyzed.

1.3 Structure of the Paper

The remainder of the paper is organized as follows: In Section 2, the investigated satellite-FSO cooperative system and corresponding channel models are introduced. The secrecy capacity performance is analyzed in Section 3 followed by the secrecy outage performance in Section 4. The analytical expressions are numerically evaluated and discussed in Section 5. Finally, summary and conclusion are drawn in Section 6.

2. System and Channel Models

In this paper, we investigate a hybrid satellite-FSO cooperative system as illustrated in Fig. 1. A satellite (S) sends confidential information to a masked destination node (D) on land with the assistance of an intermediate relay (R) situated on the ground. On the ground, an eavesdropper node (E) attempts to decode the confidential information sent from the satellite S. The long-distance communication link between the satellite S and the relay node R is an RF link modeled by the widely used Shadowed-Rician fading model. The short-distance terrestrial communication between the relay R and destination node D is through an FSO link and the channel fading follows the Gamma-Gamma distribution. Moreover, it is assumed that the channel between the satellite and relay is quasi-static, i.e., slow fading, within one symbol time interval.

2.1 Satellite Communications

In the satellite communication system, the received baseband signal after downconversion at node X, $X \in \{R, E\}$, is expressed as

$$y_X = h_X x + n, \tag{1}$$

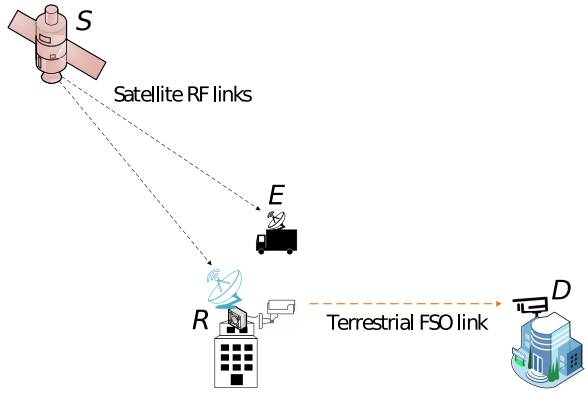

Fig. 1. The investigated hybrid satellite-FSO system consisting of a source node S (i.e., the satellite), a desired receiver D masked from satellite signals, a relay R, and an eavesdropper E.

where x is the transmitted signal with transmit power P_s, h_X represents the channel between node S and node X, n denotes the additive white Gaussian noise (AWGN) with mean zero and power spectral density N_0, which, without loss of generality, is assumed to be the same for both links. With the satellite links being modelled as Shadowed-Rician fading, the corresponding probability distribution function (PDF) $f_{|h_X|^2}(x)$ for the channel, h_X, $X \in \{R, E\}$, is given as [2]

$$f_{|h_X|^2}(x) = \alpha_X \cdot \exp(-\beta_X x) \cdot {}_1F_1(m_X; 1; \delta_X x), \quad x > 0, \tag{2}$$

where $\alpha_X = \frac{1}{2b_X}\left(\frac{2b_X m_X}{2b_X m_X + \Omega_X}\right)^{m_X}$, $\beta_X = \frac{1}{2b_X}$, $\delta_X = \frac{\Omega_X}{2b_X(2b_X m_X + \Omega_X)}$ with m_X representing the Nakagami parameter of the corresponding satellite link; and the parameters Ω_X and $2b_X$ being the average power of the LoS component and multipath component, respectively. In (2), ${}_1F_1(a, b, z)$ represents the confluent hypergeometric function of the first kind, which can be rewritten in series from the equality [19, Eq. (07.20.03.0108.01)] and the definition of Laguerre polynomial [19, Eq. (05.02.02.0001.01)] as follows:

$${}_1F_1(m_X; 1; \delta_X x) = \exp(\delta_X x) \cdot \sum_{k=0}^{m_X - 1} \frac{(1 - m_X)_k \cdot (-\delta_X x)^k}{(k!)^2}, \tag{3}$$

where $(\cdot)_k$ denotes the Pochhammer symbol [20, p. xliii].

From (2), it can be shown that the PDF and the cumulative distribution function (CDF), respectively, of the instantaneous SNR for the satellite links, i.e., $\gamma_X = \frac{P_s \mathcal{F}^2 |h_X|^2}{N_0} = \overline{\gamma}_X \cdot |h_X|^2$, $X \in \{R, E\}$, can be expressed as

$$f_{\gamma_X}(x) = \sum_{k=0}^{m_X - 1} \frac{\alpha_X (1 - m_X)_k \cdot (-\delta_X)^k \cdot x^k}{\overline{\gamma}_X^{k+1} \cdot (k!)^2} \cdot \exp(-\lambda_X x), \tag{4}$$

$$F_{\gamma_X}(x) = 1 - \sum_{k=0}^{m_X - 1} \sum_{i=0}^{k} \frac{\alpha_X \cdot (1 - m_X)_k \cdot (-\delta_X)^k \cdot x^i}{i! \cdot \lambda_X^{k-i+1} \cdot \overline{\gamma}_X^{k+1} \cdot k!} \cdot \exp(-\lambda_X x), \tag{5}$$

where $\lambda_X = \frac{\beta_X - \delta_X}{\overline{\gamma}_X}$. In (4) and (5), the average SNR $\overline{\gamma}_X = \frac{P_s \mathcal{F}^2}{N_0}$ for the satellite link between satellite S and node X, $X \in \{R, E\}$ is related to parameter $\mathcal{F}$, which denotes a scaling parameter including the effects of free space path loss, antenna pattern, etc. [21].

2.2 Terrestrial FSO Communications

For the terrestrial FSO communication link between relay R and the desired node D following the Gamma-Gamma distribution [22]. In this paper, we utilize a unified Gamma-Gamma fading

distribution, which accounts for pointing errors and type of detection techniques [23]. The PDF $f_{\gamma_D}(x)$ of the instantaneous SNR γ_D is given as [4]

$$f_{\gamma_D}(x) = \frac{\xi^2}{r\,\Gamma(\alpha)\Gamma(\beta)x} G_{1,3}^{3,0}\left(h\alpha\beta \left(\frac{x}{\mu_r}\right)^{\frac{1}{r}} \middle| \begin{matrix} \xi^2+1 \\ \xi^2,\ \alpha,\ \beta \end{matrix} \right), \tag{6}$$

where the parameter r specifies the applied detection type at the FSO receiver (i.e., $r = 1$ denotes heterodyne detection (HD) and $r = 2$ implies intensity modulation with direct detection (IM/DD)), the parameter ξ is the ratio of the equivalent beam radius to the standard deviation of the pointing error displacement (jitter) at the FSO receiver [6], the parameters α and β are used to represent the severity of fading/scintillation due to the atmospheric turbulence conditions [24], $h = \frac{\xi^2}{\xi^2+1}$, and, μ_r denotes the average electrical SNR of the FSO link under the HD or IM/DD detections (for HD detection, $\mu_1 = E[\gamma_D] = \bar{\gamma}_D$, and for IM/DD detection, $\mu_2 = \frac{\bar{\gamma}_D \alpha\beta\xi^2(\xi^2+2)}{(\alpha+1)(\beta+1)(\xi^2+1)^2}$) [4]. The expression $G_{p,q}^{m,n}\left(x \middle| \begin{matrix} a_1, \ldots, a_p \\ b_1, \ldots, b_q \end{matrix} \right)$ denotes the Meijer G-function [20, Eq. 9.343].

The CDF $F_{\gamma_D}(x)$ of the instantaneous SNR γ_D can be obtained directly from its relation with the PDF in (6) and is expressed as follows [6]:

$$F_{\gamma_D}(x) = \frac{\xi^2 r^{\alpha+\beta-2}}{(2\pi)^{r-1}\Gamma(\alpha)\Gamma(\beta)} \cdot G_{r+1,3r+1}^{3r,1}\left(\frac{(h\alpha\beta)^r}{\mu_r\, r^{2r}} x \middle| \begin{matrix} 1,\ \Delta(r, \xi^2+1) \\ \Delta(r,\ \xi^2),\ \Delta(r,\ \alpha),\ \Delta(r,\ \beta),\ 0 \end{matrix} \right), \tag{7}$$

where the notation $\Delta(k, a)$ represents that $\Delta(k, a) = \frac{a}{k}, \frac{a+1}{k}, \cdots, \frac{a+k-1}{k}$ comprising k terms. For simplicity, we adopt the following notations hereinafter: $A = \frac{\xi^2 r^{\alpha+\beta-2}}{(2\pi)^{r-1}\Gamma(\alpha)\Gamma(\beta)}$, $B = \frac{(h\alpha\beta)^r}{\mu_r\, r^{2r}}$, $\mathcal{K}_1 = \Delta(r, \xi^2+1)$, $\mathcal{K}_2 = \Delta(r, \xi^2), \Delta(r, \alpha), \Delta(r, \beta)$. Hence, the CDF $F_{\gamma_D}(x)$ can be rewritten as: $F_{\gamma_D}(x) = A \cdot G_{r+1,3r+1}^{3r,1}\left(Bx \middle| \begin{matrix} 1,\ \mathcal{K}_1 \\ \mathcal{K}_2,\ 0 \end{matrix} \right)$.

Remark 1: It is worth mentioning that another widely used distribution to model the FSO link is the Málaga model [25], [26]. However, by noticing the similarities in the distribution functions of the Málaga and Gamma-Gamma distributions, it is clear that the analytical method presented in this paper can be readily extended to the case assuming the Málaga model for the FSO link distribution. ■

Depending on the nature and complexity of the relaying technique, the relaying strategies can be generally classified into two categories, namely amplify-and-forward and decode-and-forward schemes [27]–[30]. In the AF cooperative protocol, the amplifying process by the relay node can be based on partial or full channel state information (CSI) of the link between the source and relay nodes, e.g., fixed-gain and variable-gain cooperative relaying, respectively [28]. In the following subsections, we derive the statistics of the equivalent end-to-end SNR from the source satellite to the desired destination node under the AF with fixed-gain relaying and DF relaying schemes.

2.3 Amplify-and-Forward Relaying With Fixed-Gain

With AF relaying, a fixed-gain is introduced by the node R regardless of the fading amplitude of the first hop. The corresponding end-to-end SNR γ_{eq}^{AF} at node D can be expressed as [31]

$$\gamma_{eq}^{\text{AF}} = \frac{\gamma_R \gamma_D}{\gamma_D + C}, \tag{8}$$

where C is a constant for a fixed-gain relaying [31].

The CDF $F_{\gamma_{eq}^{\text{AF}}}(x)$ of the SNR γ_{eq}^{AF} can be determined by definition as follows:

$$F_{\gamma_{eq}^{\text{AF}}}(x) = \Pr\left[\frac{\gamma_R \gamma_D}{\gamma_D + C} < x \right], \tag{9}$$

which can be further extended to

$$F_{\gamma_{eq}^{\mathrm{AF}}}(x) = \int_0^\infty \Pr\left[\gamma_R < \frac{x(\gamma_D + C)}{\gamma_D}\middle|\gamma_D\right] \cdot f_{\gamma_D}(\gamma_D)\, d\gamma_D = \int_0^\infty F_{\gamma_R}\left(\frac{x(\gamma_D + C)}{\gamma_D}\right) \cdot f_{\gamma_D}(\gamma_D)\, d\gamma_D. \tag{10}$$

Substituting (5) and (6) in (10), the CDF $F_{\gamma_{eq}^{\mathrm{AF}}}(x)$, after some algebra, can be written as

$$F_{\gamma_{eq}^{\mathrm{AF}}}(x) = 1 - \sum_{k=0}^{m_R-1}\sum_{i=0}^{k} \frac{\alpha_R (1-m_R)_k \cdot (-\delta_R)^k \cdot \xi^2 \cdot x^i}{i! \cdot \lambda_R^{k-i+1} \cdot \overline{\gamma}_R^{k+1} \cdot k! \cdot r \cdot \Gamma(\alpha)\Gamma(\beta)} \cdot \exp(-\lambda_R \cdot x)$$
$$\cdot \int_0^\infty \left(\frac{\gamma_D + C}{\gamma_D}\right)^k \cdot \frac{1}{\gamma_D} \cdot \exp\left(-\lambda_R x \cdot \frac{C}{\gamma_D}\right) \cdot G_{1,3}^{3,0}\left(h\alpha\beta\left(\frac{\gamma_D}{\mu_r}\right)^{\frac{1}{r}} \middle| \begin{matrix} \xi^2+1 \\ \xi^2,\ \alpha,\ \beta \end{matrix}\right) d\gamma_D. \tag{11}$$

Rewriting the expression $\left(\frac{\gamma_D + C}{\gamma_D}\right)^k$ in series with the binomial expansion [20, Eq. (1.111)] and utilizing the properties [19, Eqs. (01.03.26.0004.01, 07.34.21.0013.01)], the CDF in (11) can be further expressed in closed-form as follows:

$$F_{\gamma_{eq}^{\mathrm{AF}}}(x) = 1 - \sum_{k=0}^{m_R-1}\sum_{i=0}^{k}\sum_{j=0}^{i} \frac{\alpha_R \cdot \xi^2 (1-m_R)_k \cdot (-\delta_R)^k \cdot C^j \cdot \binom{i}{j} \cdot x^i \cdot \exp(-\lambda_R \cdot x)}{i! \cdot \lambda_R^{k-i+1} \cdot \overline{\gamma}_R^{k+1} \cdot r \cdot \Gamma(\alpha) \cdot \Gamma(\beta) \cdot k!}$$
$$\cdot \int_0^\infty \frac{1}{\gamma_D^{j+1}} \cdot G_{1,0}^{0,1}\left(\frac{\gamma_D}{\lambda_R x C}\middle| \begin{matrix} 1 \\ - \end{matrix}\right) \cdot G_{1,3}^{3,0}\left(h\alpha\beta\left(\frac{\gamma_D}{\mu_r}\right)^{\frac{1}{r}} \middle| \begin{matrix} \xi^2+1 \\ \xi^2,\ \alpha,\ \beta \end{matrix}\right) d\gamma_D$$
$$= 1 - \underbrace{\sum_{k=0}^{m_R-1}\sum_{i=0}^{k}\sum_{j=0}^{i} \frac{\alpha_R \cdot r^{\alpha+\beta-2} \cdot \xi^2 \cdot (1-m_R)_k \cdot (-\delta_R)^k}{(2\pi)^{r-1} \cdot \Gamma(\alpha) \cdot \Gamma(\beta) \cdot \lambda_R^{k-i+j+1} \cdot \overline{\gamma}_R^{k+1} \cdot k! \cdot j! \cdot (i-j)!}}_{\triangleq \sum_{(kij)}} \cdot x^{i-j} \cdot \exp(-\lambda_R x)$$
$$\cdot G_{r,3r+1}^{3r+1,0}\left(\frac{(h\alpha\beta)^r \lambda_R C}{\mu_r r^{2r}} x \middle| \begin{matrix} \mathcal{K}_1 \\ \mathcal{K}_2,\ j \end{matrix}\right)$$
$$= 1 - \sum_{(kij)} x^{i-j} \cdot \exp(-\lambda_R x) \cdot G_{r,3r+1}^{3r+1,0}\left(B\lambda_R C x \middle| \begin{matrix} \mathcal{K}_1 \\ \mathcal{K}_2,\ j \end{matrix}\right). \tag{12}$$

2.4 Decode-and-Forward Cooperative Relaying

The DF based relaying system is equivalent to a series network, which implies that the capacity of the system is dominated by the worst hop. Due to the fact that the channel capacity is a monotonous function of the SNR, it is straightforward to show from a capacity point of view that the equivalent SNR $\gamma_{eq}^{\mathrm{DF}}$ of the hybrid system with the DF relaying protocol is given as [27]

$$\gamma_{eq}^{\mathrm{DF}} \triangleq \min(\gamma_R, \gamma_D). \tag{13}$$

The CDF $F_{\gamma_{eq}^{\mathrm{DF}}}(x)$ of the equivalent SNR $\gamma_{eq}^{\mathrm{DF}}$ can be derived based on the definition as follows:

$$F_{\gamma_{eq}^{\mathrm{DF}}}(x) = 1 - \Pr[\min(\gamma_R, \gamma_D) > x] = 1 - \left[1 - F_{\gamma_R}(x)\right] \cdot \left[1 - F_{\gamma_D}(x)\right]. \tag{14}$$

Substituting (5) and (7) into (14), the CDF $F_{\gamma_{eq}^{\mathrm{DF}}}(x)$ can be written as

$$F_{\gamma_{eq}^{\mathrm{DF}}}(x) = 1 - \underbrace{\sum_{q=0}^{m_R-1}\sum_{l=0}^{q} \frac{\alpha_R (1-m_R)_q (-\delta_R)^q}{l! \lambda_R^{q-l+1} \overline{\gamma}_R^{q+1} q!}}_{\sum_{(ql)}} \cdot x^l \cdot \exp(-\lambda_R x)\left[1 - A \cdot G_{r+1,3r+1}^{3r,1}\left(Bx \middle| \begin{matrix} 1,\ \mathcal{K}_1 \\ \mathcal{K}_2,\ 0 \end{matrix}\right)\right]. \tag{15}$$

Remark 2: It should be noted that when the AF protocol with variable-gain scheme is employed and full CSI is utilized at the node R to counteract the instantaneous fading effects, the end-to-end SNR γ_{eq}^{V} at node D can be expressed as: $\gamma_{eq}^{\mathrm{V}} = \frac{\gamma_R \gamma_D}{\gamma_R + \gamma_D + 1} \cong \min(\gamma_R, \gamma_D) = \gamma_{eq}^{\mathrm{DF}}$ [28]. In this regard, the conducted secrecy performance analysis under the assumption of the DF relaying in this paper is also valid for the scenario of AF protocol with variable-gain relaying. ■

3. Average Secrecy Capacity Analysis

Average secrecy capacity is an important metric to evaluate the security performance of active eavesdropping. In the active eavesdropping scenario, full CSI of both the main and eavesdropper channels is available to the node S, which can adapt the achievable secrecy rate accordingly [18].

The secrecy capacity is defined as the maximum achievable perfect secrecy rate. The instantaneous secrecy capacity of the considered system is mathematically expressed as $C_s = \max\{\ln(1+\gamma_{eq}) - \ln(1+\gamma_E), 0\}$ [18]. The ASC $\overline{C}_s$ can be obtained from [6]

$$\overline{C}_s = \int_0^\infty \int_0^\infty C_s(\gamma_{eq}, \gamma_E) \cdot f_{\gamma_{eq}}(\gamma_{eq}) \cdot f_{\gamma_E}(\gamma_E)\, d\gamma_{eq} d\gamma_E = \int_0^\infty \frac{F_{\gamma_E}(\gamma)}{1+\gamma} \left[1 - F_{\gamma_{eq}}(\gamma)\right] d\gamma. \tag{16}$$

3.1 Amplify-and-Forward Relaying With Fixed-Gain

Substituting (5) and (12) into (16), the ASC $\overline{C}_s^{\mathrm{AF}}$ with the the relay node working under fixed-gain AF cooperative protocol can be expressed as

$$\overline{C}_s^{\mathrm{AF}} = \int_0^\infty \frac{1}{1+\gamma} \cdot \Bigg[1 - \underbrace{\sum_{p=0}^{m_E-1} \sum_{t=0}^{p} \frac{\alpha_E \cdot (1-m_E)_p \cdot (-\delta_E)^p}{t! \cdot \lambda_E^{p-t+1} \cdot \overline{\gamma}_E^{p+1} \cdot p!}}_{\triangleq \sum_{(pt)}} \cdot \gamma^t \cdot \exp(-\lambda_E \gamma) \Bigg]$$

$$\cdot \left[\sum_{(kij)} \gamma^{j-j} \cdot \exp(-\lambda_R \gamma) \cdot G_{r,3r+1}^{3r,0} \left(B \lambda_R C \gamma \middle| \begin{matrix} \mathcal{K}_1 \\ \mathcal{K}_2, j \end{matrix} \right) \right] d\gamma = \mathcal{I}_1 - \mathcal{I}_2, \tag{17}$$

where $\mathcal{I}_1 = \sum_{(kij)} \int_0^\infty [\gamma^{j-j} \cdot \exp(-\lambda_R \gamma) \cdot G_{r,3r+1}^{3r,0}(B\lambda_R C\gamma | \begin{smallmatrix} \mathcal{K}_1 \\ \mathcal{K}_2, j \end{smallmatrix})] \cdot \frac{1}{1+\gamma}\, d\gamma$ and $\mathcal{I}_2 = \sum_{(kij)} \sum_{(pt)} \int_0^\infty \frac{\gamma^t}{1+\gamma} \cdot \exp(-\lambda_E \gamma) \cdot [\gamma^{j-j} \cdot \exp(-\lambda_R \gamma) \cdot G_{r,3r+1}^{3r,0}(B\lambda_R C\gamma | \begin{smallmatrix} \mathcal{K}_1 \\ \mathcal{K}_2, j \end{smallmatrix})]\, d\gamma$.

Utilizing the following transformations in $\mathcal{I}_1$ and $\mathcal{I}_2$: $\frac{x^a}{1+x} = G_{1,1}^{1,1}(x | \begin{smallmatrix} a \\ a \end{smallmatrix})$, $\exp(-bx) = G_{0,1}^{1,0}(bx | \begin{smallmatrix} - \\ 0 \end{smallmatrix})$ [20, Eq. 9.3], and the solution to the integral of product of three Meijer G-functions in terms of extended generalized bivariate Meijer G-function (EGBMGF) [19, Eq. (07.34.21.0081.01)], we can obtain the exact expression for the integrals $\mathcal{I}_1$ and $\mathcal{I}_2$ as follows:

$$\begin{aligned} \mathcal{I}_1 &= \sum_{(kij)} \int_0^\infty G_{1,1}^{1,1} \left(\gamma \middle| \begin{matrix} i-j \\ i-j \end{matrix} \right) \cdot G_{0,1}^{1,0} \left(\lambda_R \gamma \middle| \begin{matrix} - \\ 0 \end{matrix} \right) \cdot G_{r,3r+1}^{3r,0} \left(B\lambda_R C\gamma \middle| \begin{matrix} \mathcal{K}_1 \\ \mathcal{K}_2, j \end{matrix} \right) d\gamma \\ &= \sum_{(kij)} \frac{1}{\lambda_R} \cdot G_{1,0:1,1:r,3r+1}^{1,0:1,1:3r+1,0} \left(\begin{matrix} 1 \\ - \end{matrix} \middle| \begin{matrix} i-j \\ i-j \end{matrix} \middle| \begin{matrix} \mathcal{K}_1 \\ \mathcal{K}_2, j \end{matrix} \middle| \frac{1}{\lambda_R}, BC \right), \end{aligned} \tag{18}$$

$$\begin{aligned} \mathcal{I}_2 &= \sum_{(kij)} \sum_{(pt)} \int_0^\infty G_{1,1}^{1,1} \left(\gamma \middle| \begin{matrix} t+i-j \\ t+i-j \end{matrix} \right) \cdot G_{0,1}^{1,0} \left((\lambda_R + \lambda_E)\gamma \middle| \begin{matrix} - \\ 0 \end{matrix} \right) \cdot G_{r,3r+1}^{3r,0} \left(B\lambda_R C\gamma \middle| \begin{matrix} \mathcal{K}_1 \\ \mathcal{K}_2, j \end{matrix} \right) d\gamma \\ &= \sum_{(kij)} \sum_{(pt)} \frac{1}{(\lambda_R + \lambda_E)} \cdot G_{1,0:1,1:r,3r+1}^{1,0:1,1:3r+1,0} \left(\begin{matrix} 1 \\ 0 \end{matrix} \middle| \begin{matrix} t+i-j \\ t+i-j \end{matrix} \middle| \begin{matrix} \mathcal{K}_1 \\ \mathcal{K}_2, j \end{matrix} \middle| \frac{1}{(\lambda_R + \lambda_E)}, \frac{BC\lambda_R}{(\lambda_R + \lambda_E)} \right). \end{aligned} \tag{19}$$

Substituting (18) and (19) into (17), the closed-form expression of the ASC for the fixed-gain AF relaying scheme is obtained. The EGBMGF function can be readily evaluated with Matlab [32].

3.2 Decode-and-Forward Cooperative Relaying

Substituting (5) and (15) into (16), the ASC $\overline{C}_s^{\mathrm{DF}}$ with the the relay node working under DF protocol or variable-gain AF protocol can be expressed as

$$\overline{C}_s^{\mathrm{DF}} = \int_0^{\infty} \frac{1}{1+\gamma} \cdot \left[1 - \underbrace{\sum_{p=0}^{m_E-1} \sum_{t=0}^{p} \frac{\alpha_E \cdot (1-m_E)_p \cdot (-\delta_E)^p}{t! \cdot \lambda_E^{p-t+1} \cdot \overline{\gamma}_E^{p+1} \cdot p!} \cdot \gamma^t}_{\triangleq \sum_{(pt)}} \cdot \exp\left(-\lambda_E \gamma\right) \right]$$

$$\cdot \underbrace{\sum_{q=0}^{m_R-1} \sum_{l=0}^{q} \frac{\alpha_R \cdot (1-m_R)_q \cdot (-\delta_R)^q}{l! \cdot \lambda_R^{q-l+1} \cdot \overline{\gamma}_R^{q+1} \cdot q!} \cdot \gamma^l}_{\triangleq \sum_{(ql)}} \cdot \exp\left(-\lambda_R \gamma\right) \cdot \left[1 - A \cdot G_{r+1,3r+1}^{3r,1}\left(B\gamma \middle| \begin{matrix} 1, \mathcal{K}_1 \\ \mathcal{K}_2, 0 \end{matrix} \right) \right] d\gamma$$

$$= \mathcal{I}_3 - \mathcal{I}_4 - \mathcal{I}_5 + \mathcal{I}_6, \tag{20}$$

where $\mathcal{I}_3 = \sum_{(ql)} \int_0^{\infty} \frac{\gamma^l}{1+\gamma} \cdot \exp\left(-\lambda_R \gamma\right) d\gamma$, $\mathcal{I}_4 = \sum_{(ql)} \int_0^{\infty} \frac{A \cdot \gamma^l}{1+\gamma} \cdot \exp\left(-\lambda_R \gamma\right) G_{r+1,3r+1}^{3r,1}\left(B\gamma \middle| \begin{matrix} 1, \mathcal{K}_1 \\ \mathcal{K}_2, 0 \end{matrix} \right) d\gamma$, $\mathcal{I}_5 = \sum_{(ql)} \sum_{(pt)} \int_0^{\infty} \frac{\gamma^{t+l}}{1+\gamma} \cdot \exp\left[-(\lambda_R + \lambda_E)\gamma\right] d\gamma$, and $\mathcal{I}_6 = \sum_{(ql)} \sum_{(pt)} \int_0^{\infty} \frac{A \cdot \gamma^{t+l}}{1+\gamma} \cdot \exp\left[-(\lambda_R + \lambda_E)\gamma\right] \cdot G_{r+1,3r+1}^{3r,1}\left(B\gamma \middle| \begin{matrix} 1, \mathcal{K}_1 \\ \mathcal{K}_2, 0 \end{matrix} \right) d\gamma$.

Utilizing the similar approach in solving the integrals $\mathcal{I}_1$ and $\mathcal{I}_2$ in Subsection 3.1, the ASC $\overline{C}_s^{\mathrm{DF}}$ can be given in closed-form as

$$\overline{C}_s^{\mathrm{DF}} = \sum_{(ql)} G_{1,2}^{2,1}\left(\lambda_R \middle| \begin{matrix} -l \\ 0, -l \end{matrix} \right) + \sum_{(ql)} A \cdot G_{1,0:1,1:r+1,3r+1}^{1,0:1,1:3r,1}\left(\begin{matrix} 1 \\ - \end{matrix} \middle| \begin{matrix} t+l \\ t+l \end{matrix} \middle| \begin{matrix} 1, \mathcal{K}_1 \\ \mathcal{K}_2, 0 \end{matrix} \middle| \frac{1}{(\lambda_R + \lambda_E)}, \frac{B}{(\lambda_R + \lambda_E)} \right)$$

$$- \sum_{(ql)} \sum_{(pt)} G_{1,2}^{2,1}\left(\lambda_R + \lambda_E \middle| \begin{matrix} -(t+l) \\ 0, -(t+l) \end{matrix} \right) - \sum_{(ql)} A \cdot G_{1,0:1,1:r+1,3r+1}^{1,0:1,1:3r,1}\left(\begin{matrix} 1 \\ - \end{matrix} \middle| \begin{matrix} l \\ l \end{matrix} \middle| \begin{matrix} 1, \mathcal{K}_1 \\ \mathcal{K}_2, 0 \end{matrix} \middle| \frac{1}{\lambda_R}, \frac{B}{\lambda_R} \right). \tag{21}$$

4. Secrecy Outage Probability Analysis

The secrecy outage probability is a useful secrecy performance metric for the scenario of passive eavesdropping, where node S does not have CSI on the eavesdropper's channel [6].

The secrecy outage probability is defined as the probability that the instantaneous secrecy capacity is below a predefined threshold rate R_s [33], i.e.,

$$SOP = \Pr\left[C_s(\gamma_{eq}, \gamma_E) \le R_s \right] = \int_0^{\infty} f_{\gamma_E}(\gamma_E) \cdot F_{\gamma_{eq}}\left((1+\gamma_E) \cdot \Theta - 1 \right) d\gamma_E, \tag{22}$$

where $\Theta = \exp\left(R_s\right) \ge 1$.

4.1 Amplify-and-Forward Relaying With Fixed-Gain

Substituting (4) and (12) into (22), the secrecy outage probability SOP^{AF} for the fixed-gain AF cooperative protocol can be expressed as

$$SOP^{\mathrm{AF}} = 1 - \int_0^{\infty} \left[\sum_{q=0}^{m_E-1} \frac{\alpha_E (1-m_E)_q \cdot (-\delta_E)^q \cdot \gamma^q}{\overline{\gamma}_E^{q+1} \cdot (q!)^2} \cdot \exp\left(-\lambda_E \gamma\right) \right] \cdot \sum_{(kij)} \left[(1+\gamma) \cdot \Theta - 1 \right]^{i-j}$$

$$\cdot \exp\left\{ -\lambda_R \cdot \left[(1+\gamma) \cdot \Theta - 1 \right] \right\} \cdot G_{r,3r+1}^{3r+1,0}\left(B\lambda_R C \cdot \left[(1+\gamma) \cdot \Theta - 1 \right] \middle| \begin{matrix} \mathcal{K}_1 \\ \mathcal{K}_2, j \end{matrix} \right) d\gamma. \tag{23}$$

In order to solve the integral in (23), we make the following change of random variables (RVs): $(1+\gamma)\Theta - 1 = x$ and $d\,x = \Theta d\,\gamma$. After some mathematical manipulations, the secrecy outage probability SOP^{AF} in (23) can be simplified as

$$SOP^{\mathrm{AF}} = 1 - \sum_{(kij)} \sum_{q=0}^{m_E-1} \frac{\alpha_E (1-m_E)_q \cdot (-\delta_E)^q}{\overline{\gamma}_E^{q+1} \cdot (q!)^2} \cdot \exp\left[-\lambda_E \left(\frac{1-\Theta}{\Theta}\right)\right] \cdot \frac{1}{\Theta} \cdot (\mathcal{I}_7 + \mathcal{I}_8), \tag{24}$$

where $\mathcal{I}_7 = \int_0^{\infty} [\frac{x+1-\Theta}{\Theta}]^q \cdot \exp\left(-\frac{\lambda_E}{\Theta} x - \lambda_R x\right) \cdot x^{i-j} \cdot G_{r,3r+1}^{3r+1,0}\left(B\lambda_R C \cdot x \middle| \begin{matrix} \mathcal{K}_1 \\ \mathcal{K}_2,\ j \end{matrix}\right) dx$ and $\mathcal{I}_8 = \int_{\Theta-1}^{0} x^{i-j} \cdot [\frac{x+1-\Theta}{\Theta}]^q \cdot \exp\left(-\frac{\lambda_E}{\Theta} x - \lambda_R x\right) \cdot G_{r,3r+1}^{3r+1,0}\left(B\lambda_R C \cdot x \middle| \begin{matrix} \mathcal{K}_1 \\ \mathcal{K}_2,\ j \end{matrix}\right) dx$.

Utilizing the following equalities: $[(1-\Theta)+x]^q = \sum_{n=0}^{q} \binom{q}{n} x^n (1-\Theta)^{q-n}$, $\exp(-bx) = G_{0,1}^{1,0}\left(bx \middle| \begin{matrix} - \\ 0 \end{matrix}\right)$, and [19, Eq. (07.34.21.0013.01)], the exact expression of the integral $\mathcal{I}_7$ can be obtained as:

$$\begin{aligned} \mathcal{I}_7 &= \sum_{n=0}^{q} \binom{q}{n} \cdot \frac{(1-\Theta)^{q-n}}{\Theta^q} \cdot \int_0^{\infty} x^{n+i-j} \cdot G_{0,1}^{1,0}\left(\left(\frac{\lambda_E}{\Theta} + \lambda_R\right) x \middle| \begin{matrix} - \\ 0 \end{matrix}\right) \cdot G_{r,3r+1}^{3r+1,0}\left(B\lambda_R C \cdot x \middle| \begin{matrix} \mathcal{K}_1 \\ \mathcal{K}_2,\ j \end{matrix}\right) dx \\ &= \sum_{n=0}^{q} \binom{q}{n} \cdot \frac{(1-\Theta)^{q-n}}{\Theta^q} \cdot \left(\frac{\lambda_E}{\Theta} + \lambda_R\right)^{-(n+i-j+1)} \cdot G_{r+1,3r+1}^{3r+1,1}\left(\frac{B\lambda_R C}{\left(\frac{\lambda_E}{\Theta} + \lambda_R\right)} \middle| \begin{matrix} -(n+i-j), \mathcal{K}_1 \\ \mathcal{K}_2,\ j \end{matrix}\right). \end{aligned} \tag{25}$$

To solve the integral $\mathcal{I}_8$, we further express the exponential term in series using the equality: $\exp(x) = \sum_{w=0}^{\infty} \frac{x^w}{w!}$ and utilize the antiderivative $\int x^{u-1} G_{p,q}^{m,n}\left(vx \middle| \begin{matrix} \mathcal{A} \\ \mathcal{B} \end{matrix}\right) dx = x^u G_{p+1,q+1}^{m,n+1}\left(vx \middle| \begin{matrix} 1-u, \mathcal{A} \\ \mathcal{B},\ -u \end{matrix}\right)$ [19, Eq. (07.34.21.0003.01)], the exact expression of the integral $\mathcal{I}_8$ can be expressed as

$$\begin{aligned} \mathcal{I}_8 &= \sum_{n=0}^{q} \binom{q}{n} \cdot \frac{(1-\Theta)^{q-n}}{\Theta^q} \sum_{w=0}^{\infty} \frac{\left[-\left(\frac{\lambda_E}{\Theta} + \lambda_R\right)\right]^w}{w!} \cdot \int_{\Theta-1}^{0} x^{w+n+i-j} \cdot G_{r,3r+1}^{3r+1,0}\left(B\lambda_R C \cdot x \middle| \begin{matrix} \mathcal{K}_1 \\ \mathcal{K}_2,\ j \end{matrix}\right) dx \\ &= \sum_{n=0}^{q} \binom{q}{n} \frac{(-1)^{n+i-j}}{\Theta^q} \sum_{w=0}^{\infty} \frac{\left(\frac{\lambda_E}{\Theta} + \lambda_R\right)^w}{w! \cdot (1-\Theta)^{-(q+w+i-j+1)}} G_{r+1,3r+2}^{3r+1,1}\left(B\lambda_R C(\Theta-1) \middle| \begin{matrix} -(w+n+i-j), \mathcal{K}_1 \\ \mathcal{K}_2,\ j, -(w+n+i-j+1) \end{matrix}\right). \end{aligned} \tag{26}$$

Substituting (25) and (26) into (24), we obtain the exact expression of SOP under fixed-gain AF relaying scheme.

4.2 Decode-and-Forward Cooperative Relaying

Substituting (4) and (15) into (22), the secrecy outage probability SOP^{DF} with the DF relaying or variable-gain AF strategies can be expressed as

$$\begin{aligned} SOP^{\mathrm{DF}} = 1 - \int_0^{\infty} &\left[\sum_{q=0}^{m_E-1} \frac{\alpha_E (1-m_E)_q \cdot (-\delta_E)^q \cdot \gamma^q}{\overline{\gamma}_E^{q+1} \cdot (q!)^2} \cdot \exp(-\lambda_E \gamma)\right] \cdot \sum_{(ql)} [(1+\gamma)\cdot\Theta - 1]^l \\ &\cdot \exp\{-\lambda_R \cdot [(1+\gamma)\cdot\Theta - 1]\} \cdot \left[1 - A \cdot G_{r+1,3r+1}^{3r,1}\left(B \cdot [(1+\gamma)\cdot\Theta - 1] \middle| \begin{matrix} 1, \mathcal{K}_1 \\ \mathcal{K}_2,\ 0 \end{matrix}\right)\right] d\gamma. \end{aligned} \tag{27}$$

The exact expression for SOP under the DF relaying can be derived by following the same procedures as in (23)–(26). Alternatively, we present an arbitrarily accurate approximation of SOP^{DF} in this subsection. Following the modified Gauss–Chebyshev quadrature technique [34], the closed-

form approximation for SOP under the DF or variable-gain AF relaying is given as

$$SOP^{\mathrm{DF}} \cong 1 - \sum_{q=0}^{m_E-1} \frac{\alpha_E (1-m_E)_q \cdot (-\delta_E)^q}{\overline{\gamma}_E^{q+1} \cdot (q!)^2} \cdot \exp\left[-\lambda_R(\Theta-1)\right] \sum_{\iota=0}^{L} w_\iota \cdot \frac{2}{t_\iota} \cdot \left(\frac{t_\iota^2}{\lambda_E + \lambda_R \Theta}\right)^{q+1} \cdot \left[\left(1 + \frac{t_\iota^2}{\lambda_E + \lambda_R \Theta}\right)\Theta - 1\right]^{l} \cdot \left[1 - A \cdot G_{r+1,3r+1}^{3r,1}\left(B\left[\left(1 + \frac{t_\iota^2}{\lambda_E + \lambda_R \Theta}\right)\Theta - 1\right] \middle| \begin{matrix} 1, \mathcal{K}_1 \\ \mathcal{K}_2, 0 \end{matrix}\right)\right], \tag{28}$$

where w_ι and t_ι, $(\iota = 1, \ldots, L)$, are the weights and abscissas of the L-order polynomial detailed in [34].

Remark 3: From the derived expressions for SOP, the probability of strictly positive secrecy capacity (SPSC) can be obtained directly by setting the target secrecy rate to zero, i.e.,

$$SPSC = \Pr\left[C_s(\gamma_{eq}, \gamma_E) \geq 0\right] = 1 - SOP|_{R_s=0}. \tag{29}$$

Therefore, by putting $R_s = 0$ (i.e., $\Theta = 1$) in the corresponding expressions for SOP, the expressions for SPSC can be directly obtained. ■

4.3 Asymptotic Secrecy Outage Probability Analysis

To provide more insights on the secrecy performance of the investigated system, we conduct asymptotic analysis on the SOP by considering very high values of the SNR γ_R.

4.3.1 Amplify-and-Forward Relaying With Fixed-Gain: We first provide the asymptotic expression for the Meijer G-function $G_{p,q}^{m,n}\left(z \middle| \begin{matrix} a_1, \ldots, a_p \\ b_1, \ldots, b_q \end{matrix}\right)$ as $z \to 0$. After rewriting the Meijer G-function in terms of the generalized hypergeometric function using the Slater's theorem [35], [36] and then utilizing the relation $\lim_{z\to 0} {}_pF_q(a_p; b_q; \pm z) \to 1$, the following asymptotic relation holds:

$$\lim_{z\to 0} G_{p,q}^{m,n}\left(z \middle| \begin{matrix} a_1, \ldots, a_p \\ b_1, \ldots, b_q \end{matrix}\right) \cong \sum_{h=1}^{m} \frac{\prod_{g=1}^{m} \Gamma(b_g - b_h)^* \cdot \prod_{g=1}^{n} \Gamma(1 + b_h - a_g)}{\prod_{g=m+1}^{q} \Gamma(1 + b_h - b_g) \cdot \prod_{g=n+1}^{p} \Gamma(a_g - b_h)} \cdot z^{b_h}, \tag{30}$$

where $(\cdot)^*$ indicates to ignore the terms when the subscript $g = h$.

Utilizing the asymptotic expressions of Meijer G-functions in (25) and (26) and after some algebra, the following asymptotic expression for the SOP can be obtained:

$$SOP^{(\mathrm{AF},\infty)} \cong 1 - \sum_{(kij)} \sum_{q=0}^{m_E-1} \frac{\alpha_E (1-m_E)_q \cdot (-\delta_E)^q}{\overline{\gamma}_E^{q+1} \cdot (q!)^2} \cdot \exp\left[-\lambda_E \left(\frac{1-\Theta}{\Theta}\right)\right] \cdot \frac{1}{\Theta^{q+1}} \cdot \left[\hat{\mathcal{I}}_7 + \hat{\mathcal{I}}_8\right], \tag{31}$$

where $\hat{\mathcal{I}}_7 = \sum_{n=0}^{q} \binom{q}{n} \cdot \mathcal{D}_1 \cdot (1-\Theta)^{q-n} \cdot \left(\frac{\lambda_E}{\Theta}\right)^{-(n+i-j+1)-b_{1,h}} \cdot (B\lambda_R C)^{b_{1,h}}$ and $\hat{\mathcal{I}}_8 = \sum_{n=0}^{q} \binom{q}{n} \cdot \mathcal{D}_2 \cdot (1-\Theta)^{q-n} \sum_{w=0}^{\infty} \frac{\left(\frac{\lambda_E}{\Theta}\right)^w}{w!} \cdot (-1)^{n+i-j} \cdot (-B\lambda_R C)^{b_{2,h}}$. In the above expressions of $\hat{\mathcal{I}}_7$ and $\hat{\mathcal{I}}_8$, $\mathcal{D}_1 = \sum_{h=1}^{3r+1} \frac{\prod_{g=1}^{3r+1} \Gamma(b_{1,g} - b_{1,h})^* \cdot \Gamma(1 + b_{1,1} - a_{1,1})}{\prod_{g=2}^{r+1} \Gamma(a_{1,g} - b_{1,h})}$ and $\mathcal{D}_2 = \sum_{h=1}^{3r+1} \frac{\prod_{g=1}^{3r+1} \Gamma(b_{2,g} - b_{2,h})^* \cdot \Gamma(1 + b_{2,1} - a_{2,1})}{\Gamma(1 + b_{2,h} - b_{2,3r+2}) \cdot \prod_{g=2}^{r+1} \Gamma(a_{2,g} - b_{2,h})}$, where $a_{1,\mu}$ and $b_{1,\nu}$ are the μ-th and ν-th term of $[-(k+n-j), \mathcal{K}_1]$ and $[\mathcal{K}_2, j]$, respectively; $a_{2,\mu}$ and $b_{2,\nu}$ represent the μ-th and ν-th term of $[-(w+n+k-j), \mathcal{K}_1]$ and $[\mathcal{K}_2, j, -(w+n+k-j+1)]$, respectively.

At very high SNR, the lowest power of γ_R in the asymptotic expression for SOP dominates the decay of the SOP, which indicates the diversity order. Hence, by observing (31), it can be concluded that the diversity order of the investigated system with respect to γ_R is $\min(1, \frac{\xi^2}{r}, \frac{\alpha}{r}, \frac{\beta}{r})$.

Remark 4: With fixed-gain AF relaying scheme, the maximum achievable secrecy diversity order of the investigated hybrid system is 1.

Remark 5: The applied detection type at the FSO receiver can potentially have a large impact on the secrecy diversity order of the hybrid satellite-FSO system with fixed-gain AF relaying scheme. The secrecy diversity order of the system employing the HD type will be twice that of using the IM/DD type under some FSO link conditions (i.e., $\xi < 1$, $\alpha < 1$, and $\beta < 1$). For some FSO fading

conditions (i.e., $\xi > \sqrt{2}$, $\alpha > 2$, and $\beta > 2$), the secrecy diversity order of the hybrid system using both FSO detection types will be the same and equal to 1. ■

4.3.2 Decode-and-Forward Cooperative Relaying: While the SNR $\gamma_R \to \infty$ (namely $\lambda_R \to 0$), the SOP in (28) can be further simplified as follows:

$$SOP^{(\mathrm{DF},\infty)} \cong 1 - \sum_{q=0}^{m_E-1} \frac{\alpha_E (1-m_E)_q \cdot (-\delta_E)^q}{\overline{\gamma}_E^{q+1} \cdot (q!)^2} \cdot \sum_{\iota=0}^{L} w_\iota \cdot \frac{2}{t_\iota} \cdot \left(\frac{t_\iota^2}{\lambda_E}\right)^{q+1} \cdot \left[\left(1+\frac{t_\iota^2}{\lambda_E}\right)\cdot\Theta - 1\right]^l$$
$$\cdot \left[1 - A \cdot G_{r+1,3r+1}^{3r,1}\left(B \cdot \left[\left(1+\frac{t_\iota^2}{\lambda_E}\right)\cdot\Theta - 1\right] \middle| \begin{matrix} 1, \mathcal{K}_1 \\ \mathcal{K}_2, 0 \end{matrix}\right)\right]. \quad (32)$$

At high SNR, it can be concluded from (32) that the asymptotic expression of SOP does not depend on the SNR γ_R. This indicates a flat curve of the SOP with respect to γ_R at high SNR.

5. Numerical Results and Discussion

In this section, we evaluate the secrecy performance of the investigated hybrid satellite-FSO system under different channel conditions for the satellite and FSO links. The satellite links are modeled as Shadowed-Rician fading channels with different shadowing severity levels: frequent heavy shadowing ($b = 0.063$, $m = 1.0$, $\Omega = 8.94 \times 10^{-4}$), average shadowing ($b = 0.126$, $m = 10.0$, $\Omega = 0.835$), and infrequent light shadowing ($b = 0.158$, $m = 19.0$, $\Omega = 1.29$) [2]. The FSO link is modeled by a unified Gamma-Gamma fading channel for weak turbulence condition ($\alpha = 2.902$, $\beta = 2.51$), moderate turbulence condition ($\alpha = 2.296$, $\beta = 1.822$), and strong turbulence condition ($\alpha = 2.064$, $\beta = 1.342$) [6]. For the AF relaying with fixed-gain scheme, the relay is set such as $C = 1$. Also, the term 'AF' specifically refers to the AF relaying with fixed gain in this Section.

5.1 Average Secrecy Capacity Performance

The impacts of the satellite and FSO channel conditions, relaying schemes, FSO detection techniques, and FSO receiver pointing errors on the ASC performance are investigated in Figs. 2(a)–2(d).

Fig. 2(a) illustrates the ASC performance under different satellite link shadowing conditions (i.e., frequent heavy shadowing and infrequent light shadowing) and FSO turbulence conditions (i.e., weak turbulence, moderate turbulence, and strong turbulence) for the considered hybrid system employing AF relaying and HD detection. It is shown in Fig. 2(a) that the ASC performance under infrequent light shadowing condition for the satellite link is significantly better than that under frequent heavy shadowing condition. This is due to the fact that severer shadowing condition for the satellite link will deteriorate the capacity performance of the hybrid system, which in return lowers the upper bound of the ASC by observing the definition of ASC. It can be also seen that the satellite shadowing severity poses significant impacts on the ASC of the hybrid system while the FSO turbulence levels have minor effects on the ASC performance of the system. This difference of impacts from the satellite and FSO link conditions is due to the small values of the fixed relay gain C in (8), which makes the end-to-end SNR of the hybrid satellite-FSO system more dependent on the SNR of the first hop than that of the second hop.

Fig. 2(b) demonstrates the ASC performance for HD and IM/DD detection techniques with the hybrid system employing AF relaying and under average shadowing satellite link condition. It can be seen that the HD detection ($r = 1$) provides slightly better ASC performance than the IM/DD detection ($r = 2$), which comes at the cost of higher level of complexity for the HD technique.

Fig. 2(c) compares the secrecy capacity performance when the relay node utilizes different relaying schemes (i.e., AF with fixed gain and DF or AF with variable gain). It is observed that when the average SNR $\overline{\gamma}_R$ is small, the performance difference between the DF and AF relayings in terms of ASC is actually small with DF relaying slightly outperforming the AF relaying. However, the AF relaying provides significantly better performance when the average SNR $\overline{\gamma}_R$ becomes larger and

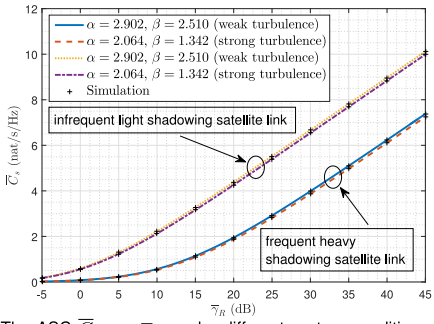

(a) The ASC $\overline{C}_s$ v.s. $\overline{\gamma}_R$ under different system conditions (AF, r = 1, $\mu_1 = 10$ dB, $\overline{\gamma}_E = -10$ dB).

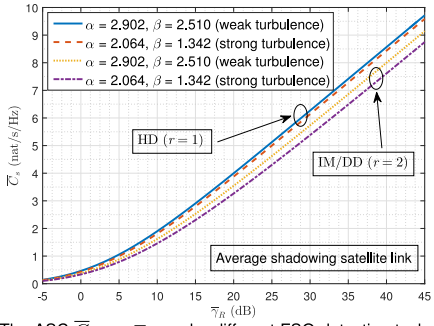

(b) The ASC $\overline{C}_s$ v.s. $\overline{\gamma}_R$ under different FSO detection techniques (AF, $\mu_r = 10$ dB, $\overline{\gamma}_E = -10$ dB).

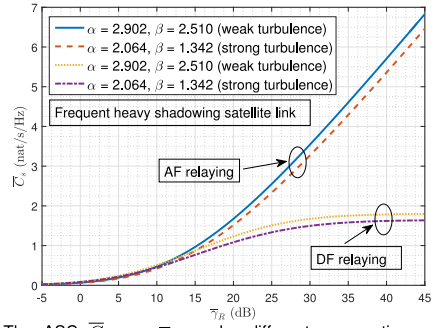

(c) The ASC $\overline{C}_s$ v.s. $\overline{\gamma}_R$ under different cooperative relaying schemes (r = 2, $\mu_2 = 10$ dB, $\overline{\gamma}_E = -10$ dB).

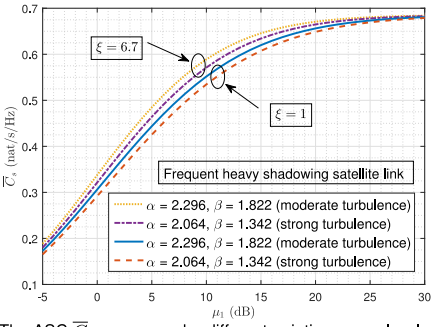

(d) The ASC $\overline{C}_s$ v.s. μ_1 under different pointing errors levels ξ (AF, r = 1, $\overline{\gamma}_R = 10$ dB, $\overline{\gamma}_E = -10$ dB).

Fig. 2. The evaluation on the ASC performance.

surpasses some threshold. This trend results from the fact that the end-to-end SNR of the hybrid system under AF relaying is mainly dominated by the SNR of the first hop while the equivalent SNR of the hybrid system with DF relaying is limited by the worst hop.

The impact of FSO receiver pointing on the ASC performance is investigated in Fig. 2(d) by considering varying levels of pointing errors ($\xi = 1$ and $\xi = 6.7$). As expected, lower level of pointing error (i.e., larger values of ξ) implies better ASC performance for the hybrid system.

5.2 Secrecy Outage Probability Performance

The impacts of the satellite and FSO channel conditions, relaying schemes, FSO detection methods, and FSO pointing errors on the secrecy diversity and SOP are illustrated in Figs. 3(a)–3(d).

Fig. 3(a) presents the SOP as a function of the average SNR μ_2 of the FSO link with IM/DD detection technique under different target secrecy rates and relaying techniques. It is obvious from Fig. 3(a) that larger values of the target rate imply worse SOP performance. It can be also observed that the hybrid system with DF relaying outperforms that with AF scheme until the average SNR of the FSO link μ_2 increases to such a threshold that the difference becomes insignificant.

In Figs. 3(b) and 3(c), the SOP is evaluated with respect to the average SNR γ_R for the hybrid satellite-FSO system under different channel conditions with AF and DF relayings, respectively. By observing the secrecy diversity with the corresponding FSO link parameters and FSO detection types in Fig. 3(b), the diversity analysis conducted in Subsection 4.3.1 and *Remark 5* is validated. It can also been seen from Fig. 3(c) that the SOP stagnates with the further increase of the SNR $\overline{\gamma}_R$ at high values of the SNR, which reaffirms the theoretical analysis in Subsection 4.3.2.

Fig. 3(d) displays the SOP as a function of the average SNR $\overline{\gamma}_E$ of the eavesdropper link under different FSO link conditions and relaying techniques. It can be seen that under the same channel condition, the DF relay based system provides better performance when the SNR $\overline{\gamma}_E$ is low while the opposite is true when the SNR becomes larger.

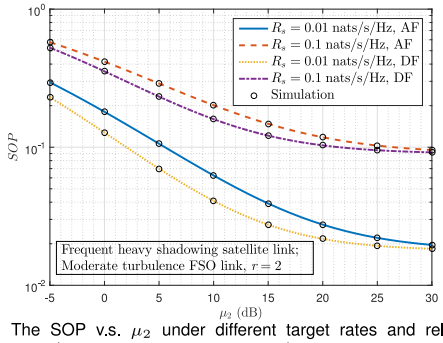

(a) The SOP v.s. μ_2 under different target rates and relaying schemes ($\overline{\gamma}_R = 10$ dB, $\overline{\gamma}_E = -10$ dB).

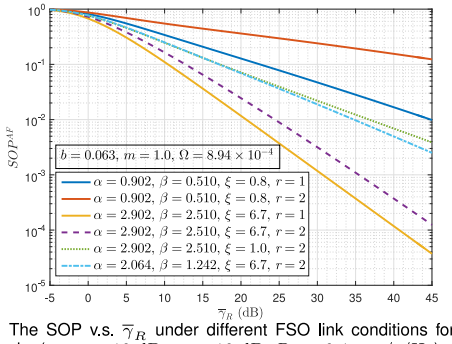

(b) The SOP v.s. $\overline{\gamma}_R$ under different FSO link conditions for AF relaying($\overline{\gamma}_E = -10$ dB, $\mu_r = 10$ dB, $R_s = 0.1$ nat/s/Hz).

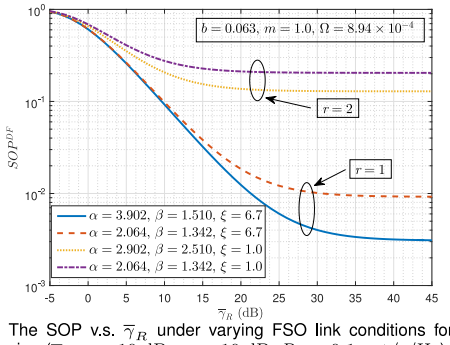

(c) The SOP v.s. $\overline{\gamma}_R$ under varying FSO link conditions for DF relaying ($\overline{\gamma}_E = -10$ dB, $\mu_r = 10$ dB, $R_s = 0.1$ nat/s/Hz).

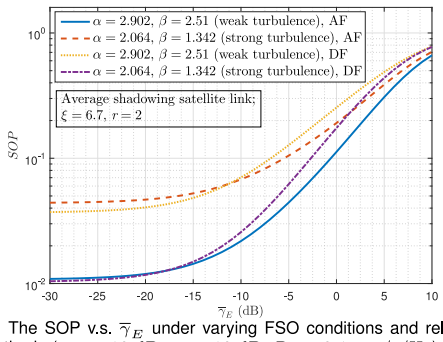

(d) The SOP v.s. $\overline{\gamma}_E$ under varying FSO conditions and relaying methods ($\overline{\gamma}_D = 10$ dB, $\mu_r = 10$ dB, $R_s = 0.1$ nat/s/Hz).

Fig. 3. The evaluation on the SOP performance.

6. Conclusions

In this paper, the secrecy performance of a hybrid satellite-FSO system was investigated. The exact expressions for the ASC and SOP were derived under both AF and DF relaying schemes and validated through simulations. The secrecy diversity analysis was also conducted to provide more insights on the investigated system. It is found that the satellite link conditions pose a larger impact on the secrecy performance of the hybrid system than the FSO link for both the AF and DF based systems. However, for the DF based system, the secrecy diversity is zero with respect to the SNR of the legitimate satellite link while the secrecy diversity depends on both the FSO link conditions and the FSO detection techniques for the AF based hybrid system.

References

[1] R. Radhakrishnan, W. W. Edmonson, F. Afghah, R. M. Rodriguez-Osorio, F. Pinto, and S. C. Burleigh, "Survey of inter-satellite communication for small satellite systems: Physical layer to network layer view," *IEEE Commun. Surveys Tuts.*, vol. 18, no. 4, pp. 2442–2473, May 2016.

[2] M. R. Bhatnagar and M. Arti, "Performance analysis of hybrid satellite-terrestrial FSO cooperative system," *IEEE Photon. Technol. Lett.*, vol. 25, no. 22, pp. 2197–2200, Nov. 2013.

[3] R. Li, "Towards a New Internet for the Year 2030 and Beyond," 2018. [Online]. Available: https://www.itu.int/en/ITU-T/Workshops-and-Seminars/201807/Documents/3_Richard%20Li.pdf. Accessed on: Aug. 16, 2018.

[4] E. Zedini, I. S. Ansari, and M.-S. Alouini, "Performance analysis of mixed Nakagami-*m* and Gamma–Gamma dual-hop FSO transmission systems," *IEEE Photon. J.*, vol. 7, no. 1, Feb. 2015, Art. no. 7900120.

[5] E. Balti and M. Guizani, "Mixed RF/FSO cooperative relaying systems with co-channel interference," *IEEE Trans. Commun.*, vol. 66, no. 9, pp. 4014–4027, Sep. 2018.

[6] H. Lei, Z. Dai, I. S. Ansari, K. Park, G. Pan, and M.-S. Alouini, "On secrecy performance of mixed RF-FSO systems," *IEEE Photon. J.*, vol. 9, no. 4, Aug. 2017, Art. no. 7904814.

[7] H. Lei, H. Luo, K.-H. Park, Z. Ren, G. Pan, and M.-S. Alouini, "Secrecy outage analysis of mixed RF-FSO systems with channel imperfection," *IEEE Photon. J.*, vol. 10, no. 3, Jun. 2018, Art. no. 7904113.

[8] E. Leitgeb *et al.*, "Hybrid wireless networks combining WLAN, FSO and satellite technology for disaster recovery," in *Proc. IST Mobile Wireless Commun. Summit*. Dresden, Germany: IST, Feb. 2005, pp. 1–5.

[9] International Telecommunication Union (ITU), "ITU Facts and Figures," 2017. [Online]. Available: https://www.itu.int/en/ITU-D/Statistics/Documents/facts/ICTFactsFigures2017.pdf. Accessed on: Aug. 16, 2018.

[10] K. An, M. Lin, J. Ouyang, and W.-P. Zhu, "Secure transmission in cognitive satellite terrestrial networks." *IEEE J. Sel. Areas Commun.*, vol. 34, no. 11, pp. 3025–3037, Nov. 2016.

[11] K. An, T. Liang, X. Yan, and G. Zheng, "On the secrecy performance of land mobile satellite communication systems," *IEEE Access*, vol. 6, pp. 39606–39620, 2018.

[12] M. J. Saber and S. M. S. Sadough, "On secure free-space optical communications over Málaga turbulence channels," *IEEE Wireless Commun. Lett.*, vol. 6, no. 2, pp. 274–277, Apr. 2017.

[13] A. D. Wyner, "The wire-tap channel," *Bell Syst. Techn. J.*, vol. 54, no. 8, pp. 1355–1387, Oct. 1975.

[14] L. Yang, T. Liu, J. Chen, and M.-S. Alouini, "Physical-layer security for mixed η-μ and $\mathcal{M}$-distribution dual-hop RF/FSO systems," *IEEE Trans. Veh. Technol.*, vol. 67, no. 12, pp. 12427–12431, Oct. 2018.

[15] Q. Huang, M. Lin, K. An, J. Ouyang, and W.-P. Zhu, "Secrecy performance of hybrid satellite-terrestrial relay networks in the presence of multiple eavesdroppers," *IET Commun.*, vol. 12, no. 1, pp. 26–34, Dec. 2017.

[16] Z. Lin, M. Lin, J.-B. Wang, Y. Huang, and W.-P. Zhu, "Robust secure beamforming for 5G cellular networks coexisting with satellite networks," *IEEE J. Sel. Areas Commun.*, vol. 36, no. 4, pp. 932–945, Apr. 2018.

[17] B. Li, Z. Fei, X. Xu, and Z. Chu, "Resource allocations for secure cognitive satellite terrestrial networks," *IEEE Wireless Commun. Lett.*, vol. 7, no. 1, pp. 78–81, Feb. 2018.

[18] Y. Ai, M. Cheffena, A. Mathur, and H. Lei, "On physical layer security of double Rayleigh fading channels for vehicular communications," *IEEE Wireless Commun. Lett.*, vol. 7, no. 6, pp. 1038–1041, Dec. 2018.

[19] The Wolfram Functions Site. [Online]. Available: http://functions.wolfram.com/. Accessed on: August 6, 2018.

[20] I. S. Gradshteyn and I. M. Ryzhik, *Table of Integrals, Series, and Products*, 7th ed. Burlington, MA, USA: Academic, 2007.

[21] K. Guo, M. Lin, B. Zhang, J. Ouyang, and W.-P. Zhu, "Secrecy performance of satellite wiretap channels with multi-user opportunistic scheduling," *IEEE Wireless Commun. Lett.*, vol. 7, no. 6, pp. 1054–1057, Dec. 2018, doi: 10.1109/LWC.2018.2859385.

[22] B. Makki, T. Svensson, M. Brandt-Pearce, and M.-S. Alouini, "On the performance of millimeter wave-based RF-FSO multi-hop and mesh networks," *IEEE Trans. Wireless Commun.*, vol. 16, no. 12, pp. 7746–7759, Dec. 2017.

[23] I. S. Ansari, F. Yilmaz, and M.-S. Alouini, "Performance analysis of FSO links over unified Gamma-Gamma turbulence channels," in *Proc. IEEE Veh. Technol. Conf.*. Glasgow, UK: IEEE, Jul. 2015, pp. 1–5.

[24] E. Zedini, H. Soury, and M.-S. Alouini, "On the performance analysis of dual-hop mixed FSO/RF systems," *IEEE Trans. Wireless Commun.*, vol. 15, no. 5, pp. 3679–3689, May 2016.

[25] I. S. Ansari, F. Yilmaz, and M.-S. Alouini, "Performance analysis of free-space optical links over Málaga ($\mathcal{M}$) turbulence channels with pointing errors," *IEEE Trans. Wireless Commun.*, vol. 15, no. 1, pp. 91–102, Jan. 2016.

[26] P. Saxena, A. Mathur, M. R. Bhatnagar, and Z. Ghassemlooy, "BER of an optically pre-amplified FSO system under Málaga turbulence, pointing errors, and ASE noise," in *Proc. IEEE Ann. Int. Symp. Pers., Indoor, Mobile Radio Commun.*. Montreal, Canada: IEEE, Oct. 2017, pp. 1–6.

[27] Y. Ai and M. Cheffena, "On multi-hop decode-and-forward cooperative relaying for industrial wireless sensor networks," *Sensors*, vol. 17, no. 4, pp. 1–21, Mar. 2017.

[28] M. O. Hasna and M.-S. Alouini, "End-to-end performance of transmission systems with relays over Rayleigh-fading channels," *IEEE Trans. Wireless Commun.*, vol. 2, no. 6, pp. 1126–1131, Nov. 2003.

[29] A. Mathur, M. R. Bhatnagar, Y. Ai, and M. Cheffena, "Performance analysis of a dual-hop wireless-power line mixed cooperative system," *IEEE Access*, vol. 6, pp. 34380–34392, 2018.

[30] Y. Ai and M. Cheffena, "Performance analysis of hybrid-ARQ with chase combining over cooperative relay network with asymmetric fading channels," in *Proc. IEEE Veh. Technol. Conf.*. Montreal, Canada: IEEE, Sep. 2016, pp. 1–6.

[31] G. K. Karagiannidis, "Performance bounds of multihop wireless communications with blind relays over generalized fading channels," *IEEE Trans. Wireless Commun.*, vol. 5, no. 3, pp. 498–503, Mar. 2006.

[32] H. Chergui, M. Benjillali, and S. Saoudi, "Performance analysis of project-and-forward relaying in mixed MIMO-pinhole and Rayleigh dual-hop channel," *IEEE Commun. Lett.*, vol. 20, no. 3, pp. 610–613, Mar. 2016.

[33] A. Mathur, Y. Ai, M. R. Bhatnagar, M. Cheffena, and T. Ohtsuki, "On physical layer security of α-η-κ-μ fading channels," *IEEE Commun. Lett.*, vol. 22, no. 10, pp. 2168–2171, Oct. 2018.

[34] N. Steen, G. Byrne, and E. Gelbard, "Gaussian quadratures for the integrals $\int_0^\infty e^{-x^2} f(x)\,dx$ and $\int_0^b e^{-x^2} f(x)\,dx$," *Math. Compu.*, vol. 23, no. 107, pp. 661–671, 1969.

[35] K. Roach, "Meijer G function representations," in *Proc. Int. Symp. Symbolic Algebraic Comput.* Hawaii, USA: ACM, Jul. 1997, pp. 205–211.

[36] M. R. Bhatnagar and Z. Ghassemlooy, "Performance analysis of Gamma–Gamma fading FSO MIMO links with pointing errors," *J. Lightw. Technol.*, vol. 34, no. 9, pp. 2158–2169, May 2016.